# Evaluation of Performance Characteristics of a Switched-Capacitor Buck-Boost PFC Converter-Fed Sensorless BLDCM Drive

**V. Aishwarya** and **K. Gnana Sheela**

**Abstract** This paper details a switched-capacitor buck-boost (SCBB) converter for correcting the power factor of a sensorless brushless DC motor (BLDCM) drive. SCBB converter is typically preferred for correction of power factor at the input AC side. Drive speed control is achieved using the voltage mode control of the power factor correction (PFC) converter. This control technique requires only one voltage sensor for its operation and regulates the motor speed by changing the converter's DC-link voltage. The inverter supplying the motor is operated at the supply frequency by digitally commutating the BLDCM, minimizing the switching power losses in inverter switches. Discontinuous conduction mode (DCM) of operation is employed in this converter to attain a power factor of one at the supply mains. Direct back-EMF (BEMF) zero-crossing detection (ZCD) technique is employed for the sensorless motor control. It is a sensorless method that eliminates position sensors and thus makes the drive system compact and economical. Drive performance is analyzed using the converter for a broad speed range. A power factor of 0.9999 is obtained at the AC side, with enhanced power quality metrics inside the IEEE 519-2014 standard's approved tolerance range.

**Keywords** Brushless DC motor (BLDCM) · Back-EMF (BEMF) zero-crossing detection (ZCD) · Discontinuous conduction mode (DCM) · Sensorless control · Switched-capacitor buck-boost (SCBB) converter · Voltage mode control · Power factor correction (PFC)

## 1 Introduction

BLDCM drives find numerous applications in aerospace applications, HVAC, industrial tools, motion control, hybrid electric vehicles, household utilities like washing machines, refrigerators, water pumps, blowers, mixers, and so on because of their advantages like high efficiency, rugged nature, enormous power per unit volume,

V. Aishwarya (✉) · K. Gnana Sheela
APJ Abdul Kalam Technological University, Trivandrum 695016, India

rapid dynamic response, longer operational life, silent operation, more extensive speed ranges, and a larger torque-to-weight ratio [1–4]. It is a special-electric motor with back-EMF (BEMF) and current waveforms with trapezoidal and quasi-rectangular shapes. It comprises a stator with concentrated windings and a rotor made of permanent magnets [2–4]. The brush absentia in the motor permits electronic current commutation in the motor phases based on rotor position feedback. Hence, BLDCMs incorporate sensors to identify the instantaneous position of the rotor that increases the motor size and expense and decreases its sturdiness [1, 3, 5–8]. Expense and efficiency are the two constraints for the implementation of lower power BLDCM drives. Drive economization is achieved by two methods: the topological method and control method. The least switch count is utilized in the topological method to implement the power circuit, whereas novel control techniques are developed to obtain the control method's expected performance [3, 4, 9, 10]. Hence, several sensorless control strategies were reported to improve drive performance. It involves the variable inductance method, BEMF ZCD, variation of flux-linkage, extended Kalman filter (EKF) method, and MRAS control [3, 5, 8, 11–15].

In traditional motor drives, a full-bridge uncontrolled rectifier and a large DC-bus capacitor supply the motor. This topology draws a highly distorted source current from the input AC supply. It results in a low power factor (PF) and a large crest factor (CF) [2–4, 11, 16]. The power quality metrics are far above the tolerable range set by IEEE 519-2014 standards. Hence, power factor correction (PFC) converters are required to obtain a PF of one at the input side [3, 4, 10, 11, 16, 17]. PFC converters commonly have two working modes: (i) continuous conduction mode (CCM), (ii) discontinuous conduction mode (DCM) [2–4, 9, 11, 17]. CCM offers continuous inductor current and decreased converter switching stresses but needs many sensors. CCM is commonly used for high-power applications. On the other hand, DCM needs just one sensor for measuring the DC-link voltage and provides discontinuous inductor current DCM has higher switching stresses on the converter's switch and is confined to lower power applications only [2–4, 9, 11, 16]. The SCBB converter highlights features like a fast dynamic response, compact capacitors, and enhanced light-load performance [1, 18]. This paper describes an SCBB PFC converter-based sensorless BLDCM drive. The inverter's switches work at the supply frequency through the digital commutation the motor, thereby decreasing the switching power losses associated with the inverter switches [2, 4, 11]. The drive speed is adjusted by modifying the DC voltage using the voltage mode control in the proposed drive [3].

The organization of the paper is as follows: Sect. 2 deals with the drive schematic; Sects. 3 and 4 describe the working of the SCBB converter and drive control. Section 5 describes the Simulation results and discussions, and Sect. 6 presents the conclusion of the paper.
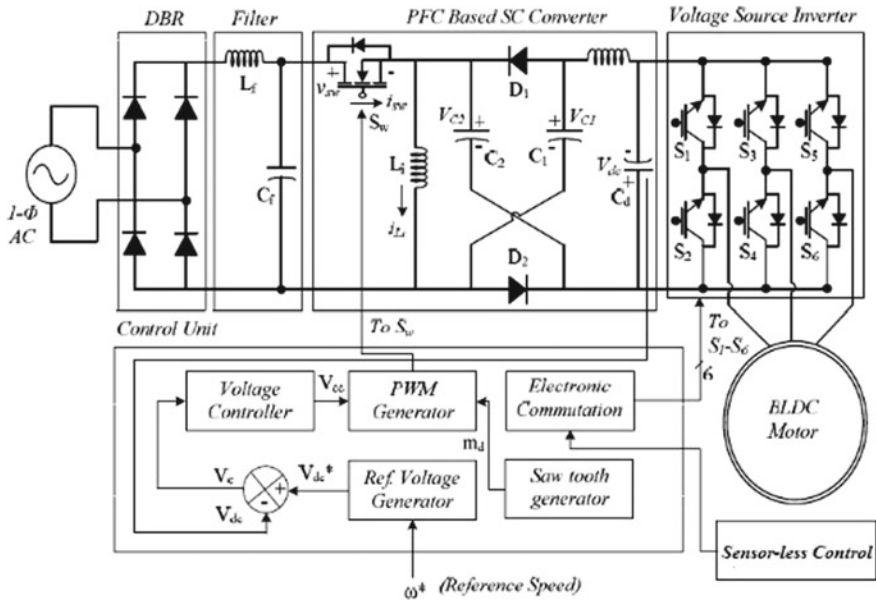
**Fig. 1** Schematic of SCBB converter-based sensorless BLDCM drive

## 2 Drive Schematic

The proposed SCBB converter-based drive comprises a single-phase SCBB converter, voltage-source inverter, and a BLDCM. Figure 1 depicts the schematic of an SCBB converter-based sensorless BLDCM drive. An SCBB converter is connected to an uncontrolled rectifier bridge to achieve a controlled voltage output. The LC-filter at the rectifier output eliminates electromagnetic interference issues and current ripples. The converter's DC-link voltage is regulated using the voltage mode control. The converter works in discontinuous conduction mode (DCM) to economize and simplify the drive's control section [2–4, 11]. The Sensorless BEMF ZCD scheme is utilized for the electronic drive commutation [5, 7, 13–15, 18, 19]. Here, the BEMFs of the motor phases are utilized to develop gating pulses for the inverter's switches. It does not need additional sensors to detect the instantaneous rotor position and thus economize the drive system [3, 5, 7, 13, 14, 18, 19].

## 3 Working of SCBB Converter

The functioning of the SCBB converter in DCM is explained in this section. The SCBB converter operates in DCM, where the current $i_{Li}$ of the input inductor becomes discontinuous in one switching cycle. Figure 2a–c represent the modes of operation
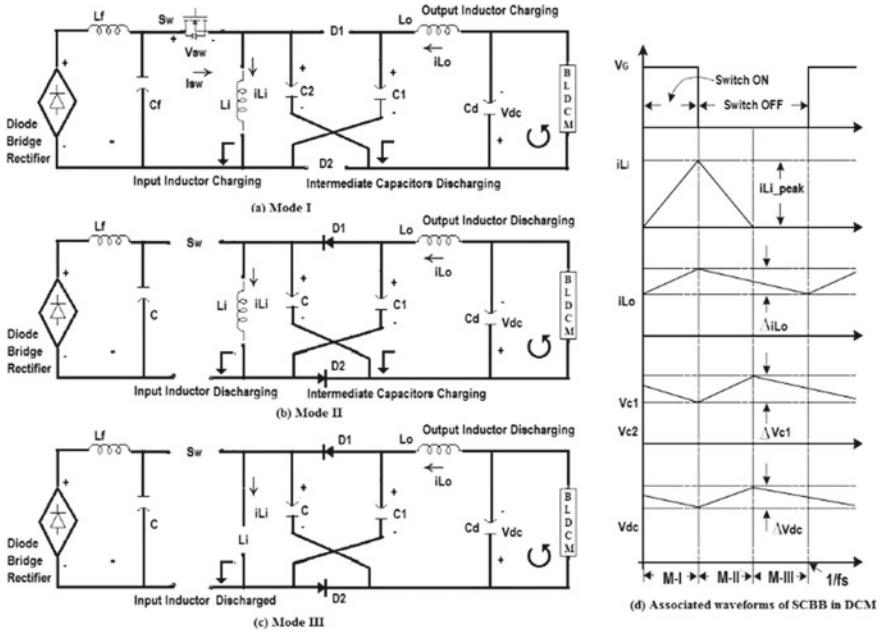
**Fig. 2** Working modes of SCBB converter and associated waveforms

of the SCBB converter, and Fig. 2d depicts the corresponding waveforms associated with it [1, 11].

Mode I: The input and the output inductors, Li and Lo, begin to charge when the switch Sw is energized. The capacitors C1 and C2 begin to discharge, as depicted in Fig. 2a.

Mode II: The diodes D1, D2 start conducting when the switch Sw is de-energized. The inductors Li and Lo, begin to discharge through the diodes. The intermediary capacitors C1, C2 begin to charge, as depicted in Fig. 2b.

Mode III: During this period, the input inductor, Li, discharges entirely and remains at zero. The output inductor, Lo, maintains discharging, as portrayed in Fig. 2c. The output capacitor, Cd, meets the energy-requirement of the BLDCM [3].

## 4 Drive Control System

BLDCM drive control is categorized into two sections: SCBB converter control for regulating the DC-link voltage and PFC, and BLDCM control to obtain digital commutation [2–4].

## 4.1 SCBB Converter Control: Voltage Mode Control

In voltage mode control, a set DC voltage ($V_{dc}^*$) proportionate to a specific set speed ($N^*$) is developed [2–4, 20]:

$$V_{dc}^* = k_{v^*} N^* \tag{1}$$

where $k_v$ is back-EMF (BEMF) constant, and $N^*$ is the desired motor set speed.

The original DC-link voltage is reduced from the generated set voltage to produce an error voltage, $V_{err}$ [3]. At any instant '$n$,' the error voltage is:

$$V_{err}(n) = V_{dc}^*(n) - V_{dC}(n) \tag{2}$$

The error voltage is provided to a PI controller to develop a regulated voltage output, $V_{cd}$ as:

$$V_{cd}(n) = V_{err}(n-1) + k_{vp} * \{V_{err}(n) - V_{err}(n-1)\} + k_{vi} * V_{err}(n) \tag{3}$$

where $k_{vp}$ and $k_{vi}$ represent the PI controller gains. Lastly, the regulated voltage output ($V_{cd}$) is juxtaposed with a carrier wave of large frequency, $m_d(t)$, to make firing signals for the converter's switch [1–4, 11].

$$m_d(t) < V_{cd}(t), \text{ then } S_w = 1, \text{ else } S_w = 0 \tag{4}$$

where $S_w$ represents the gating signal for the converter switch.

## 4.2 Sensorless BLDCM Control

Sensored BLDCM control necessitates hall-effect sensors to determine the rotor's position each 60° for each phase's efficient current commutation. The sensors increase the drive system's bulkiness and expense [3, 11]. A sensorless BLDCM control technique is employed in the proposed work, making the drive system compact and economical. It is based on identifying the switching instant when the un-energized phase's BEMF crosses zero [4, 6–8, 14–16, 19]. The zero- crossing is utilized to generate the gating sequence. The BEMF of a phase is measured when it crosses zero when that phase is un-energized. The phase voltage of that un-energized phase is equal to the neutral voltage [11]. The zero-crossing point is to be shifted 30° electrical in phase to derive the gating sequence [4, 6]. As the neutral-point voltage is not physically available for these motors, this voltage signal can be regenerated in software by determining the arithmetic mean of the values of three simultaneously sampled BEMF signals, as given by Eq. (5). The redeveloped motor-neutral voltage is then compared to each BEMF signal to identify the zero-crossing events. The

zero-crossing point is achieved when the BEMF signals are equal to this regenerated motor-neutral-point voltage [21].

$$V_n = (e_a + e_b + e_c)/3 \qquad (5)$$

where $V_n$ is the motor-neutral voltage, $e_a$, $e_b$, and $e_c$ are BEMF voltages of phases $a$, $b$, and $c$.

## 5 Simulation Results and Discussions

The Simulink package of MATLAB software is used to conduct the simulation of the proposed drive. The drive response is analyzed for various speeds, motor loads, and source voltages. Motor parameters, including the rotor speed ($N$), electromagnetic BEMF ($e_a$), torque ($T_e$), and motor current ($i_a$), are studied for the evaluation of the drive response. The converter parameters, including the DC-link voltage, capacitor voltages, and inductor currents, are investigated to study the SCBB converter's behavior. Power quality metrics like source current distortion and power factor are observed. The maximum voltage and current stresses on the switch of the SCBB converter are determined to fix the ratings of the switch. Table 1 depicts the simulation circuit parameters of the SCBB converter [1].

**Steady-state performance of the drive**. Figure 3a depicts the response when the drive operates in steady state at rated conditions. The source current, almost concurring with the source voltage, affirms the operation at a very high power factor of 0.9999. The discontinuity in the input inductor current demonstrates the discontinuous operation of the SCBB converter. The maximum voltage and current stresses on the switch of the SCBB converter are 500 V and 24 A.

**Table 1** Simulation circuit parameters of SCBB converter-based BLDCM drive

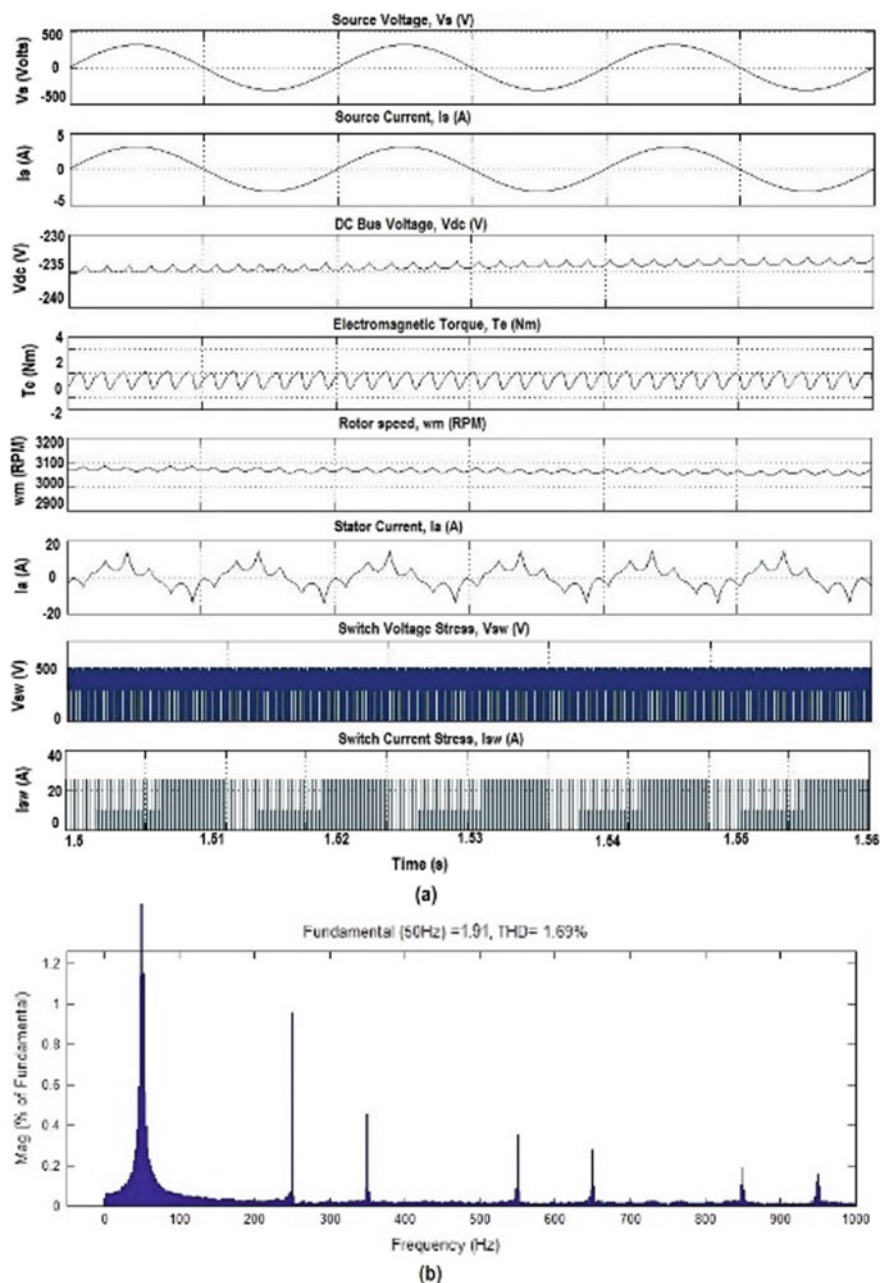| S. No. | Circuit parameter | Value |
|---|---|---|
| 1 | Input AC voltage, $V_{in}$ | 198 V |
| 2 | DC-link voltage, $V_{dc}$ | 120 V |
| 3 | Input inductor, $L_i$ | 250 μH |
| 4 | Output inductor, $L_o$ | 5 mH |
| 5 | Intermediary capacitors, $C_1$ and $C_2$ | 0.5 μF |
| 6 | DC-link capacitor, $C_d$ | 2200 μF |
| 7 | Filter capacitor, $C_f$ | 330 nF |
| 8 | Filter inductor, $L_f$ | 4 mH |
| 9 | BLDCM | 4 pole, 2000 rpm, 250 W |

**Fig. 3** **a** Steady-state response of SCBB converter-based drive, **b** harmonic spectrum of source current

It is observed from Fig. 3b that, at steady-state conditions, the current distortion of source current is 1.69%.

**Dynamic performance of the drive**. The dynamic drive response is studied from the following observations made during (i) a sudden DC-link voltage variation at starting, (ii) sudden DC-link voltage variation at speed-control operation, (iii) sudden load-torque variation. Drive response during a variation in the source voltage is analyzed [3, 11]. Figures 4, 5, 6, and 7 portray the dynamic drive response while starting with the sudden DC-link voltage variation from 0 to 75 V; speed control with a sudden DC-link voltage variation from 100 to 150 V; during a sudden load-torque variation to 0.8 Nm from 0.4 Nm, and a sudden dip in AC voltage to 180 V from 270 V, respectively. When $V_{dc}$ is gradually varied over the entire operational range, an excellent performance is obtained in the drive. The drive returns to its steady state very rapidly in 75 ms after the occurrence of the voltage fluctuation. Tables 2 and 3 represent the drive responses during speed control and AC voltage variations,
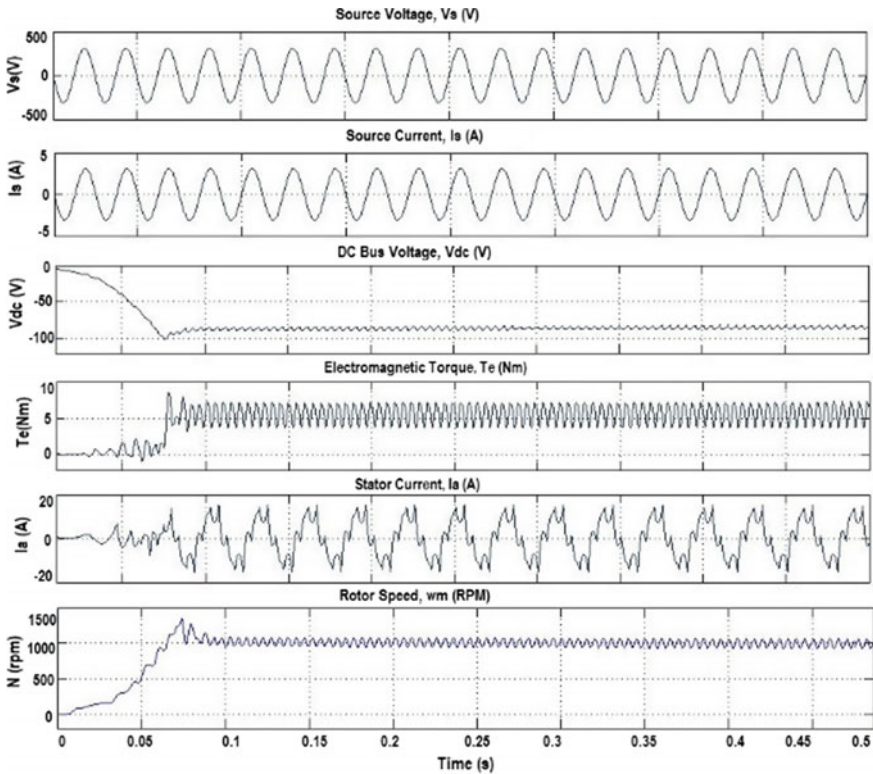


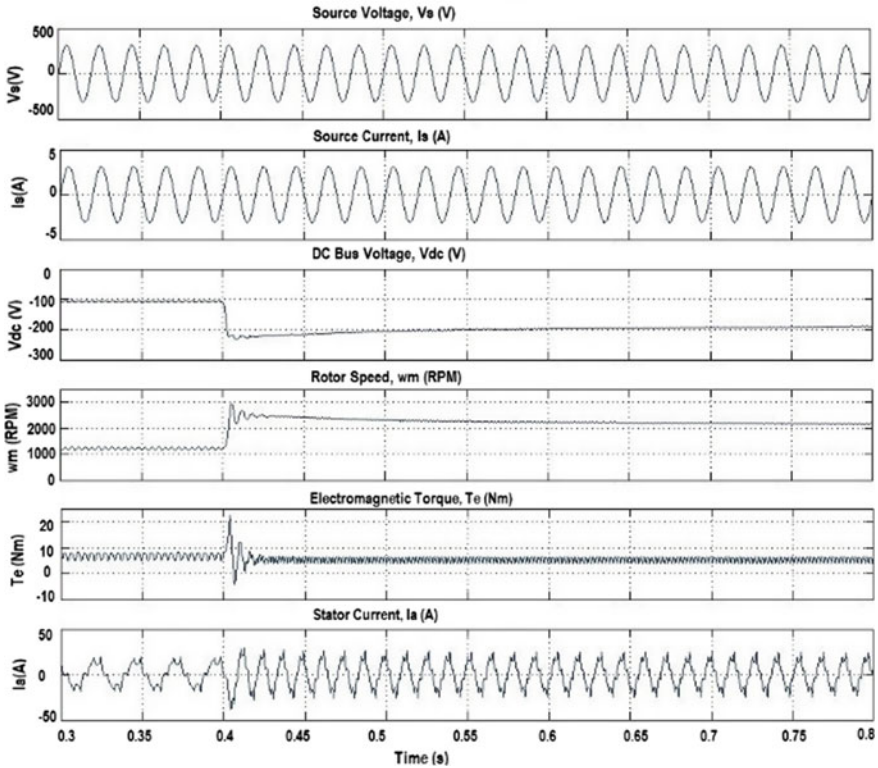**Fig. 4** Dynamic response of SCBB converter-based drive during starting

**Fig. 5** Dynamic response of SCBB converter-based drive during speed control

respectively. It is found that the input current distortion is below 5% in both cases, at all times.

# 6 Conclusion

This paper described the performance analysis of the switched-capacitor buck-boost (SCBB) converter-based BLDCM drive. Voltage mode control is employed to obtain closed-loop drive speed control. Inverter power losses are decreased by switching the inverter at the supply frequency through electronic BLDCM commutation. The sensorless BEMF ZCD method is employed for gating pulse generation for the inverter switches. Since hall-effect position sensors are eliminated, the drive is more compact, economical, and has improved efficiency. The maximum voltage and current stresses on the SCBB converter switch are 500 V and 24 A, respectively,
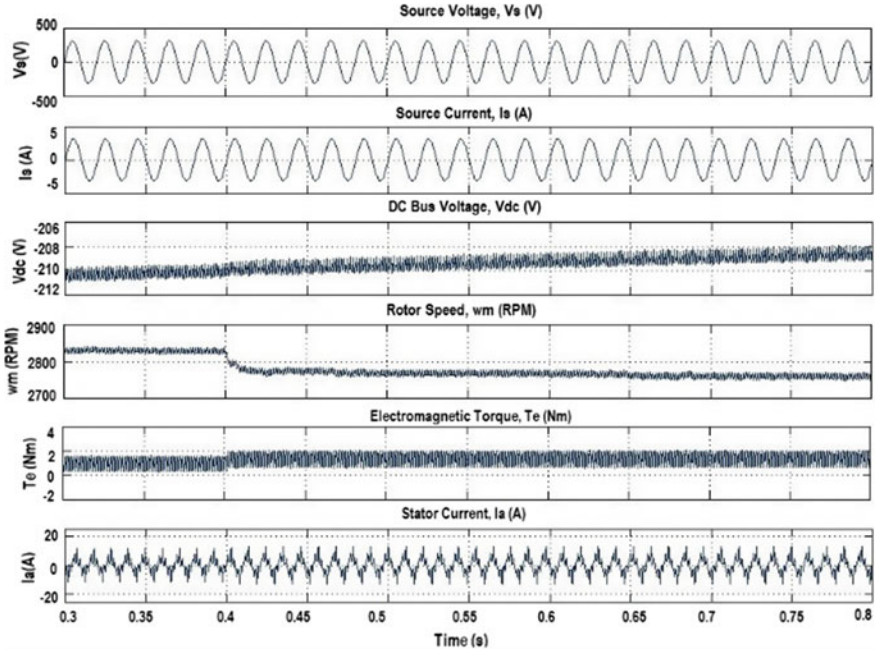
**Fig. 6** Dynamic response of SCBB converter-based drive during a sudden load-torque variation

within the switch ratings' safe limits. A power factor of 0.9999 is obtained due to the DCM operation of the converter. The power quality metrics obtained fall inside the tolerable range of the IEEE 519-2014 standard.
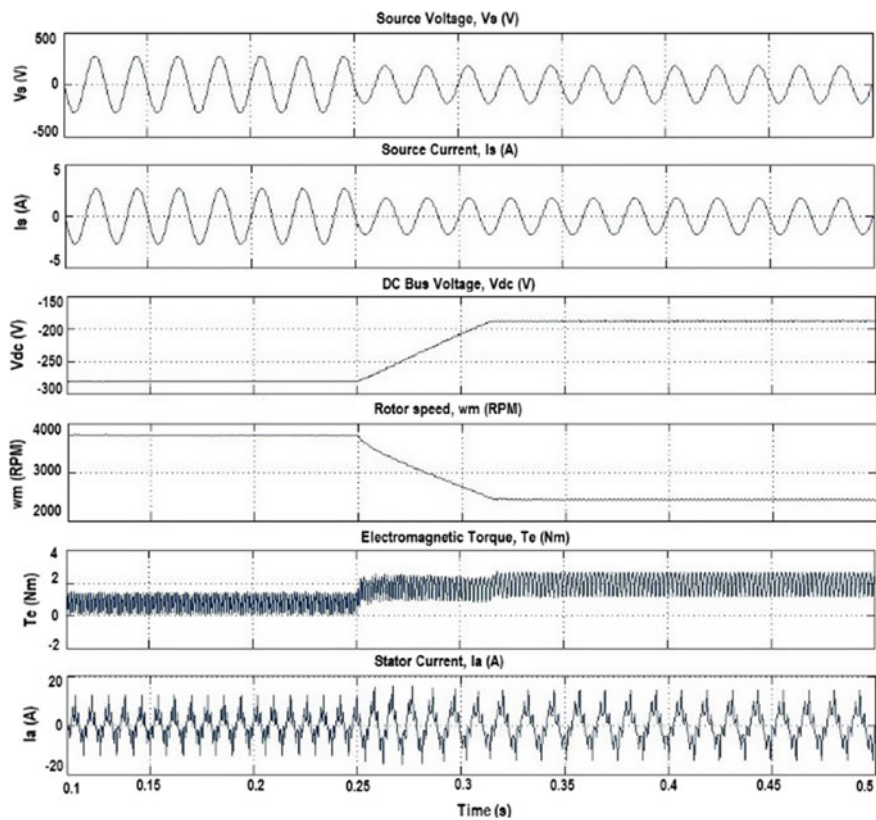
**Fig. 7** Dynamic response of SCBB converter-based drive during source voltage fluctuation

**Table 2** Drive performance during speed control

| S. No. | $V_{dc}$ (V) | Speed (in rpm) | THD of $i_s$ (%) | Power factor | Source current, $i_s$ (A) |
|---|---|---|---|---|---|
| 1 | 75 | 550 | 4.83 | 0.9943 | 0.57 |
| 2 | 100 | 945 | 4.64 | 0.9978 | 0.75 |
| 3 | 120 | 1000 | 4.51 | 0.9980 | 0.87 |
| 4 | 160 | 1600 | 4.21 | 0.9990 | 1.12 |
| 5 | 180 | 1890 | 4.07 | 0.9995 | 1.34 |

**Table 3** Drive performance during supply voltage fluctuations

| S. No. | $V_s$ (V) | THD of $i_s$ (%) | Power factor | Source current, $i_s$ (A) |
|---|---|---|---|---|
| 1 | 180 | 3.4 | 0.9995 | 1.95 |
| 2 | 200 | 3.55 | 0.9991 | 1.90 |
| 3 | 240 | 3.80 | 0.9983 | 1.82 |
| 4 | 240 | 3.80 | 0.9983 | 1.82 |
| 5 | 260 | 4.07 | 0.9979 | 1.77 |
| 6 | 270 | 4.12 | 0.9975 | 1.72 |

# References

1. B. Singh, V. Bist, A PFC based switched-capacitor buck-boost converter fed BLDC motor drive, in *2013 Annual IEEE India Conference, INDICON 2013* (2013)
2. V. Bist, B. Singh, PFC Cuk converter-fed BLDC motor drive. IEEE Trans. Power Electron. **30**, 871–887 (2015). https://doi.org/10.1109/TPEL.2014.2309706
3. V. Aishwarya, K. Gnana Sheela, Performance analysis of Buck-Boost and Cuk converter-fed brushless DC motor drives. Mater. Today Proc. 1865–1873 (2019)
4. S. Singh, B. Singh, Power factor correction in permanent magnet brushless DC motor drive using single-phase Cuk converter. J. Eng. Sci. Technol. **5**, 412–425 (2010)
5. P.P. Acarnley, J.F. Watson, Review of position-sensorless operation of brushless permanent-magnet machines. IEEE Trans. Ind. Electron. **53**, 352–362 (2006)
6. B. Singh, S. Singh, State of the art on permanent magnet brushless DC motor drives. J. Power Electron. **9**, 1–17 (2009)
7. D. Montesinos, S. Galceran, F. Blaabjerg et al., Sensorless control of PM synchronous motors and brushless DC motors. An overview and evaluation, in *2005 European Conference on Power Electronics and Applications* (IEEE Computer Society, Dresden, Germany, 2005), pp. 1–10
8. V. Aishwarya, B. Jayanand, Estimation and control of sensorless brushless DC motor drive using extended Kalman filter, in *Proceedings of IEEE International Conference on Circuit, Power and Computing Technologies, ICCPCT 2016* (Institute of Electrical and Electronics Engineers Inc., 2016)
9. B. Singh, S. Singh, Single-phase power factor controller topologies for permanent magnet brushless DC motor drives. IET Power Electron. **3**, 147–175 (2010). https://doi.org/10.1049/iet-pel.2008.0313
10. B. Singh, B.N. Singh, A. Chandra et al., A review of single-phase improved power quality AC-DC converters. IEEE Trans. Ind. Electron. **50**, 962–981 (2003). https://doi.org/10.1109/TIE.2003.817609
11. V. Aishwarya, K. Gnana Sheela, An integrated single-stage converter-fed sensor-less motor drive. Int. J. Recent Technol. Eng. **8**, 21–25 (2019). https://doi.org/10.35940/ijrte.A1185.078219
12. D. Lenine, B.R. Reddy, S.V. Kumar, Estimation of speed and rotor position of BLDC motor using extended Kalman filter, in *IET Seminar Digest, IET-UK International Conference on Information and Communication Technology in Electrical Sciences (ICTES 2007)* (IET, Tamil Nadu, India, 2007), pp. 433–440
13. F. Hicham, R. Abdellatif, D. Mohamed, Sensorless control of the trapezoidal BLDCM using sliding mode observer, in *IFAC Proceedings Volumes (IFAC-PapersOnline)* (IFAC, Prague, Czech Republic, 2005), pp. 83–88
14. T.H. Kim, H.W. Lee, M. Ehsani, State of the art and future trends in position sensorless brushless DC motor/generator drives, in *31st Annual Conference of IEEE Industrial Electronics Society, 2005. IECON 2005* (IEEE, Raleigh, NC, USA, 2005), pp. 1718–1725

15. N. Matsui, Sensorless PM brushless DC motor drives. IEEE Trans. Ind. Electron. **43**, 300–308 (1996). https://doi.org/10.1109/41.491354
16. O. García, J.A. Cobos, R. Prieto et al., Single phase power factor correction: a survey. IEEE Trans. Power Electron. **18**, 749–755 (2003). https://doi.org/10.1109/TPEL.2003.810856
17. B. Singh, V. Bist, Power factor correction (PFC) converters feeding brushless DC motor drive. Int. J. Eng. Sci. Technol. **7**, 65–75 (2015)
18. B. Singh, Recent advances in permanent magnet brushless DC motors. Sadhana **22**, 837–853 (1997). https://doi.org/10.1007/BF02745848
19. C.S. Joice, S.R. Paranjothi, V.J.S. Kumar, Digital control strategy for four-quadrant operation of three phase BLDC motor with load variations. IEEE Trans. Ind. Inf. **9**, 974–982 (2013). https://doi.org/10.1109/TII.2012.2221721
20. M. Jacob, V. Aishwarya, Sensorless brushless DC motor drive fed by Cuk converter, in *Proceedings of IEEE International Conference on Circuit, Power and Computing Technologies, ICCPCT 2016* (Institute of Electrical and Electronics Engineers Inc., Nagercoil, India, 2016)
21. D. Torres, Sensorless BLDC control with back-EMF filtering using a majority function, AN1160 (2008)